551.515.21

# On the balance of forces and radial accelerations in hurricanes

By W. M. GRAY
*Colorado State University, Fort Collins*

(Manuscript received 18 July 1961; in revised form 9 April 1962)

SUMMARY

The degree to which the gradient or cyclostrophic wind equation is applicable for hurricane winds above the surface friction layer is tested on 10 levels in four hurricanes (8 different days) in which aircraft of the National Hurricane Research Project of the United States Weather Bureau flew radial leg penetrations during the 1957-58 seasons. All 10 levels flown were between 6,000 and 16,000 ft altitude and each level had six or more radial leg penetrations except one that had five. Application of the cylindrical radial equation of motion is made for the constant-pressure levels flown. Results show that there is lack of radial balance by a wide margin between pressure gradient, centrifugal and Coriolis forces. Evaluation of the local and advective changes of the substantial derivative only partly makes up for this lack of balance. It is therefore necessary to postulate the existence of internal radial friction, both in an instantaneous fixed-coordinate system and in one that moves with the storm centre. This residual radial friction averages 25 to 30 per cent of the pressure-gradient force. As a consequence, the gradient wind equation in both cyclindrical and in natural coordinates is invalid. Also, steady-state or deepening hurricanes must have stronger pressure gradients than corresponding centrifugal and Coriolis accelerations. Comments on the possible mechanism for this internal friction are given.

## 1. INTRODUCTION

Hurricanes have often been described as vortices in which the cyclostrophic wind equation should be valid in the core of maximum winds and the gradient wind equation in the periphery. But the degree to which these equations really describe the balance of forces has not been determined. This has been due to lack of reliable wind and pressure-height information. With the installation of the National Hurricane Research Project of the United States Weather Bureau in 1956, and with technical development of the gyro-navigation system and other instruments, these observational inadequacies have been reduced and to some extent overcome. The Doppler navigation system has given for the first time accurate wind data over ocean areas. Within the limits of accuracy of observations, the questions concerning the form of the laws of motion applicable in hurricanes can now be answered in certain respects for several storms which were thoroughly covered by research missions of the National Hurricane Research Project.

This paper presents a first attempt to take up some special aspects of the balance of forces computed from the flight data. Computations are made for Atlantic hurricanes *Carrie* (1957), *Cleo* (1958), *Daisy* (1958), and *Helene* (1958).

### (*a*) *Instrumentation of aircraft*

During the hurricane seasons of 1957-1958, the National Hurricane Research Project operated three aircraft in conjunction with the U.S. Air Force. There were two B-50's and one B-47. The instrumentation installed and maintained in these planes has been described by Hillary and Christensen (1957). It will therefore suffice to note that the instrumentation of interest for this study consisted of a Doppler (gyro) Navigation wind measurement, radio and pressure altimeter for determination of the altimeter correction ($D$), and a vortex thermometer for temperature measurements. Punch-card systems were installed in the back of the aircraft. Instantaneous values of the above parameters were punched at specified time intervals – one card every two to ten seconds – with the more rapid punching in the hurricane cores. These punch-cards were taken to National Hurricane Research Project after each mission and evaluated by machine processing. Note was taken of the hurricane displacement over the duration of the mission and all quantities were plotted in a latitude-longitude coordinate system fixed with respect to the storm centre.

In this study, use is made of the horizontal winds and the observed $D$ values.

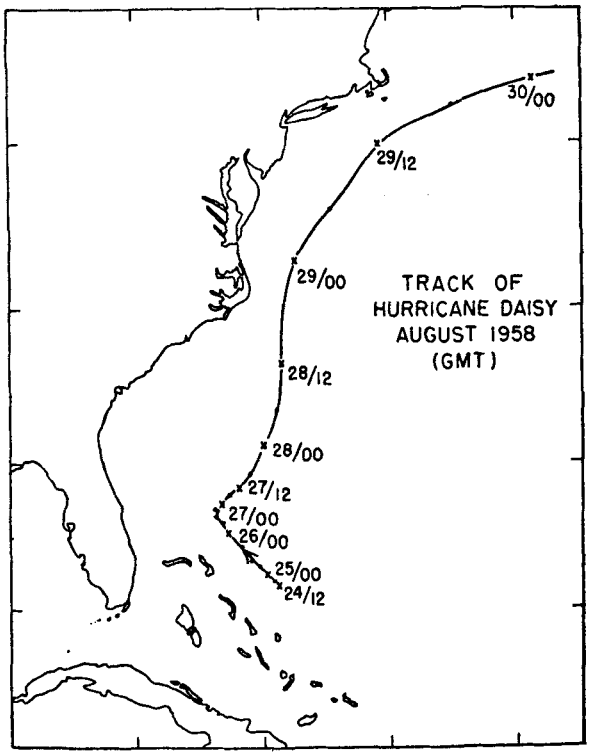


Figure 1. Track of hurricane *Daisy*, August 1958 (GMT).

### (*b*) *Missions in hurricane Daisy (1958)*

Hurricane *Daisy* began to form on 24 August, just to the north-east of the Bahama Islands (Fig. 1). By 1200 GMT, 25 August, the maximum winds in the core were 70 kt. It was at this time that National Hurricane Research Project aircraft first entered *Daisy*. One Air Force B-50 made radial penetrations into the eye at 830 mb; additional legs were executed at 1,600 and 2,800 ft. The second B-50 operated in the middle troposphere at 570 mb. The B-47 aircraft carried out a mission in and around the storm at 237 mb.

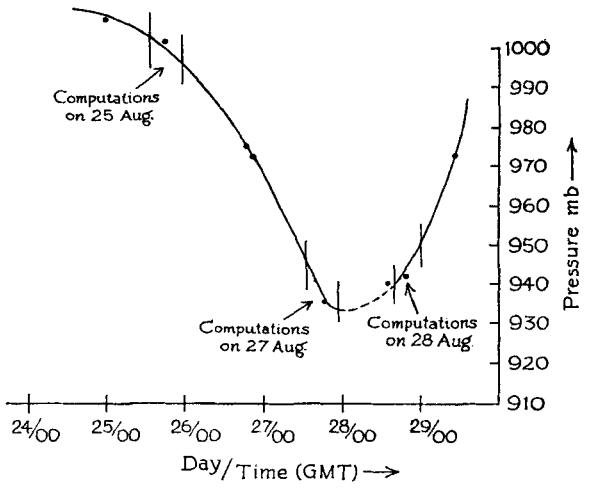


Figure 2. Central pressure with time/date for hurricane *Daisy*.

Two missions were flown into *Daisy* on 26 August, but without radial penetration. On 27 and 28 August, radial penetrations were made at 630 and 620 mb respectively. *Daisy* reached its peak intensity on 27 August, with maximum winds at one flight level above 115 kt. A plot of central pressure with time is given in Fig. 2.

### (c) *Mission into hurricane Cleo (1958)*

Hurricane *Cleo* formed in an easterly wave, west of the Canary Islands, on 9 August. It moved steadily W for six days to approximately 15°N, 48°W, and then turned N moving steadily in this direction until it took on extra-tropical characteristics SE of Newfoundland on 19 August. It reached maximum intensity on 14th August, just before turning northward. The maximum winds were approximately 120 kt and minimum pressure 945 mb. A three-plane National Hurricane Research Project mission was flown into the storm on 18 August when *Cleo* was moving in an approximately steady state towards NNE at 14 kt. Maximum winds were approximately 95 kt and minimum pressure 970 mb. The storm eye was nearly 25 miles in diameter and the eye wall-clouds quite extensive. One mission was accomplished at 820 mb, another at 580 mb, and a third at 255 mb (see storm track, Fig. 3).

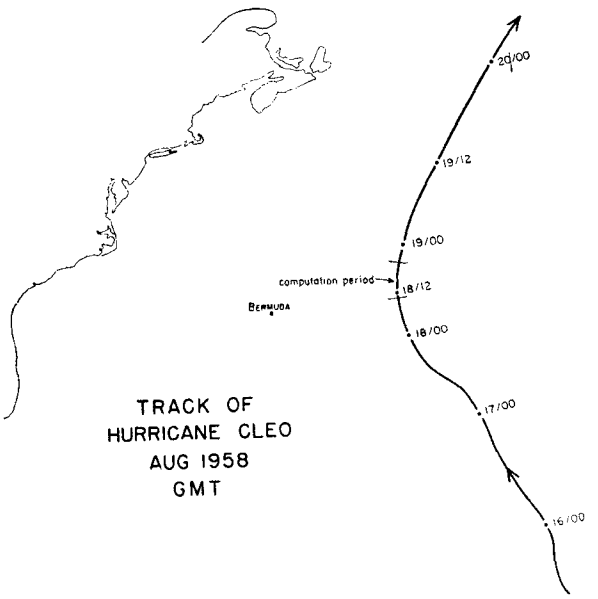


Figure 3. Track of hurricane *Cleo*, August 1958 (GMT).

### (d) *Missions into hurricane Carrie (1957)*

Hurricane *Carrie* formed from an easterly wave near 20°N, 35°W, on 5 September. It moved steadily W and NW. By 15 September it was located at 30°N, 58°W moving to NW at 12 kt in approximate steady-state. Its central pressure was 965 mb and maximum winds 85 kt. A mid-tropospheric probe (605 mb) was made at this time. Another mid-tropospheric flight into *Carrie* (690 mb) was made on 17 September when the storm had changed direction and was moving towards ENE at 13 kt. Minimum pressure and maximum winds were nearly the same as on 15 September (see storm track, Fig. 4).

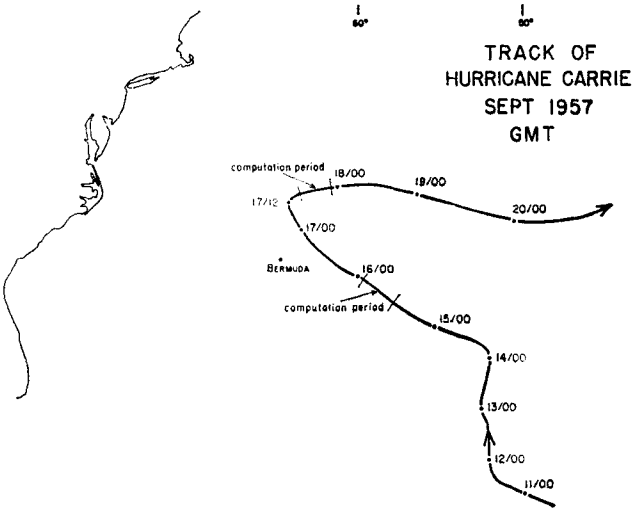


Figure 4. Track of hurricane *Carrie*, September 1957 (GMT).

### (e) *Missions in hurricane Helene (1958)*

This storm started to developed on 22 September at 22°N, 65°W, or 200 naut. mi. NNE of San Juan, P.R. It moved almost directly NW for the next four days, while slowly intensifying (see storm track, Fig. 5). A flight at 635 mb was made on 24 September when the central pressure was approximately 995 mb and maximum winds were 60 kt.

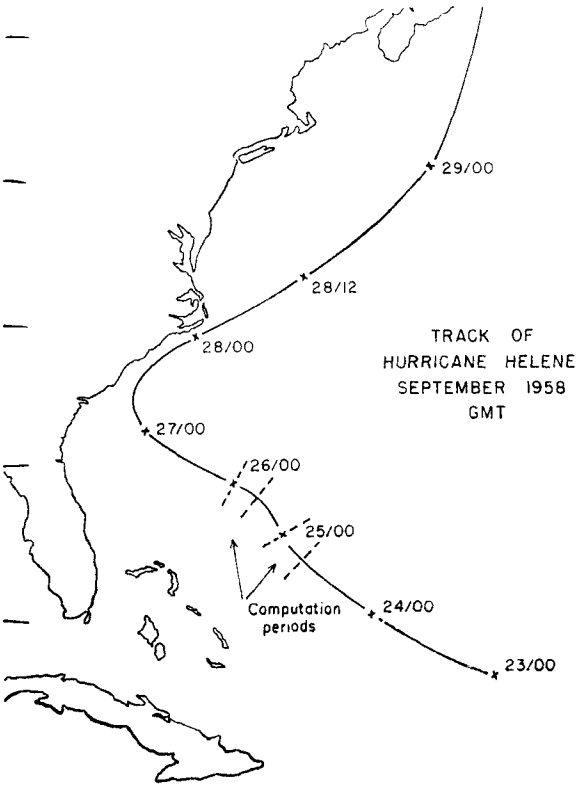


Figure 5. Track of hurricane *Helene*, September 1958 (GMT).

Another flight was made on 25 September at 810 mb when the storm's central pressure was approximately 980 mb and maximum winds approximately 80 kt. Other flights into *Helene* were made by National Hurricane Research Project on 26 September. Only the results of the two flights on 24 and 25 September are presented in this paper.

Each day's data was collected in six to ten hours between the approximate hours of 1400 to 2400 GMT. For computational purposes, an essentially steady state must be assumed for this period of flight, even though some changes could be noted when aircraft repeatedly passed the same point with respect to the storm centre.

Table 1 contains the storms, levels, dates, maximum winds, etc. for which computations were performed. These 10 levels are those where at least six radial legs were flown (except *Cleo* 820 mb which had five radial legs). It is at these levels where field analysis of computed values could be made. A typical sample of a flight path along one of these levels is shown in Fig. 10.

TABLE 1. LEVELS TO WHICH RADIAL ACCELERATION COMPUTATIONS WERE MADE

| Storm | Date | Pressure level (mb) | Approx. max. wind at flight level (kt) | Approx. central pressure (mb) | Central pressure change | Storm direction | Speed (kt) |
|---|---|---|---|---|---|---|---|
| | 1958 | | | | | | |
| *Daisy* | 25 August | 830 | 60 | 990 | deepening | 320 | 7 |
| | 25 August | 570 | 60 | 990 | deepening | 320 | 7 |
| | 27 August | 630 | 120 | 940 | deepening then steady | 030 | 8 |
| | 28 August | 620 | 105 | 945 | filling rapidly | 010 | 18 |
| | 1957 | | | | | | |
| *Carrie* | 15 September | 605 | 85 | 965 | steady | 310 | 12 |
| | 17 September | 690 | 95 | 970 | steady | 080 | 13 |
| | 1958 | | | | | | |
| *Cleo* | 18 August | 820 | 90 | 970 | steady | 015 | 14 |
| | 18 August | 580 | 85 | 970 | steady | 015 | 15 |
| | 1958 | | | | | | |
| *Helene* | 24 September | 635 | 60 | 995 | deepening | 320 | 10 |
| | 25 September | 810 | 80 | 980 | deepening | 310 | 6 |

The hurricane's central pressures were obtained from aircraft dropsondes within the storm's eye. The aircraft were able to accomplish radial-flight penetrations by inspection of the radar-cloud bands and from close scrutiny of the Doppler-determined winds.

## 2. EQUATIONS OF MOTION AND COMPUTATIONAL PROCEDURE

Aircraft observations, of necessity, are taken in a mixed space-time coordinate system. But, as previously stated, usually the complexity of the reference frame can be reduced by the assumption (usually valid in the first approximation) that the storm remains in essentially steady state for the duration of a flight mission. Granted this premise, all observations can be assigned a location in a coordinate system fixed with respect to the moving centre. Given a plot of the data in this form, an investigation of the forces and

accelerations present may be provided from a variety of viewpoints. Three of the most common approaches are :

(1). Computation of the actual forces with respect to the instantaneous centre position along the radial and tangential axis of a polar coordinate system.

(2). A similar computation in a moving reference frame where at first the translatory storm velocity is subtracted from all winds, so that the wind field studied is that relative to the moving centre.

(3). Computations in a natural coordinate system in which the forces acting on individual air particles are determined.

System No. 3, a Lagrangian one, is in some respects the most attractive. But computations depend on knowledge of the radius of trajectory curvature, a quantity which is not measured but must be obtained by indirect means based on the field distribution of data. In such a procedure the shortcomings of the steady-state assumption and of the frequent wide gaps between flight legs are essential.

Now in hurricanes, much interest reasonably centres on the radial accelerations since they are related to the mass flow through the system and have the energy releases which produce and maintain these cyclones. Given the objective of investigating these accelerations, the first two coordinate systems are not subject to the difficulties encountered in the natural frame, and so all requisite data are furnished by single radial flight legs of perhaps 15-min duration and the whole job can be done by machine process if desired. In contrast, calculations along the tangential direction not only give less promise of insight into the hurricane but they are also difficult to accomplish since airplanes cannot fly circles around hurricanes and since gradients of wind and pressure usually are very weak along this axis compared to the radial axis.

Since the course to be pursued will be to determine whatever is possible about radial accelerations, most calculations will be made with respect to the disturbance's centre position since it is felt that the greatest importance resides in the radial coordinates.

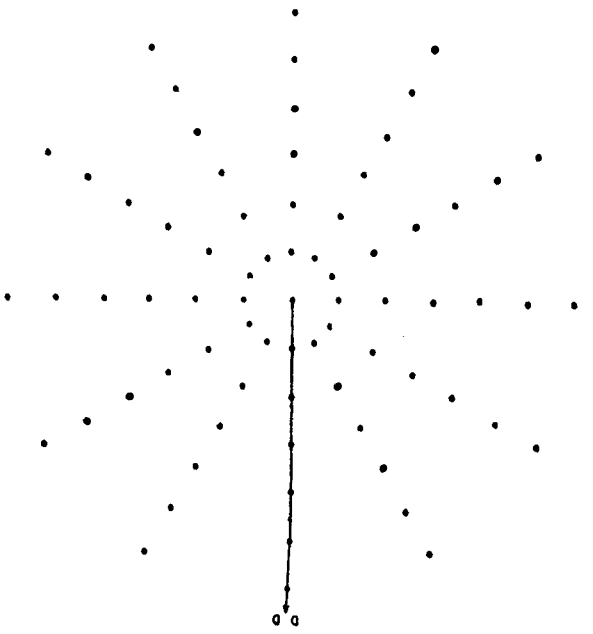

Figure 6. Grid used in computations.

Later, however, the transformation to moving coordinates will be made as there is the advantage that local time changes are eliminated, and advective changes are then referred to the storm's centre rather than to a point fixed on earth.

The polar coordinate system will be applied to constant-pressure surfaces which then are treated as quasi-horizontal surfaces, where it may be noted that even in the areas with strongest pressure gradient the slope of a constant pressure surface will not exceed the order of 1 : 100 (pressure gradient of 2 mb mile$^{-1}$). The radius $r$ will be positive outward and the polar angle $\theta$ positive counterclockwise. Given the horizontal velocity components $v_r$ and $v_\theta$ along $r$ and $\theta$, the altimeter correction $D$, the acceleration of gravity $g$, and the time $t$, the cylindrical equations of motion are :

$$\dot{v}_r = \frac{v_\theta^2}{r} + fv_\theta - g\,\partial D/\partial r + F_r \quad . \quad . \quad . \quad (1)$$

$$\dot{v}_\theta = -\frac{v_\theta v_r}{r} - fv_r - g\frac{\partial D}{r\partial\theta} + F_\theta \quad . \quad . \quad . \quad (2)$$

Here the dot denotes substantial time differentiation and $F_r$ and $F_\theta$ are the components of the frictional force along $r$ and $\theta$, respectively. $\dot{v}_r$ is positive when directed outward along $r$. Only the first of these two equations will be treated in view of the preceding statement of objective.

Given $\dot{v}_r = 0$, $F_r = 0$, a type of gradient wind balance along $r$ may be defined to be given by

$$\frac{\frac{v_\theta^2}{r} + fv_\theta}{g\frac{\partial D}{\partial r}} = 1 \quad . \quad . \quad . \quad . \quad . \quad (3)$$

Defining $$\dot{v}_r)_{gr} = \dot{v}_r - F_r \quad . \quad . \quad . \quad . \quad . \quad (4)$$

Eq. (1) may be written

$$\dot{v}_r)_{gr} = \frac{v_\theta^2}{r} + fv_\theta - g\frac{\partial D}{\partial r} \quad . \quad . \quad . \quad . \quad (5)$$

The first calculation will be concerned with the question to what extent $\dot{v}_r)_{gr}$ and also $fv_\theta$ may be neglected compared to the centrifugal and pressure gradient terms. This calculation was performed only for flight legs which were radial or which departed little from the radial direction. This restriction would not be required for storms with tangential symmetry. Such symmetry, however, was not observed.

### (*a*) *Computational procedure*

The computational procedure begins with the plotting of $v_\theta$ and of $D$ values vs. radius on graph paper and the drawing of smooth curves of best fit through the data points (Figs. 7 and 8). Scattering of individual values was not great and representative curves were obtained in all cases for $v_\theta$; however, there remained some leeway in drawing the $D$ profiles, especially close to the centre.

Next, the curves of $v_\theta$ and $D$ were divided into finite radial intervals starting at 5 naut. mi. from the centre, going outward. Integrating from $r_1$ to $r_2$ where $r_2 > r_1$, $g\int_{r_1}^{r_2} dD/dr\ dr = g\,(D_2 - D_1)$ where the total derivative has been substituted for the partial derivative. This is permissible since only a one-dimensional equation with $r$ as independent variable is being solved.

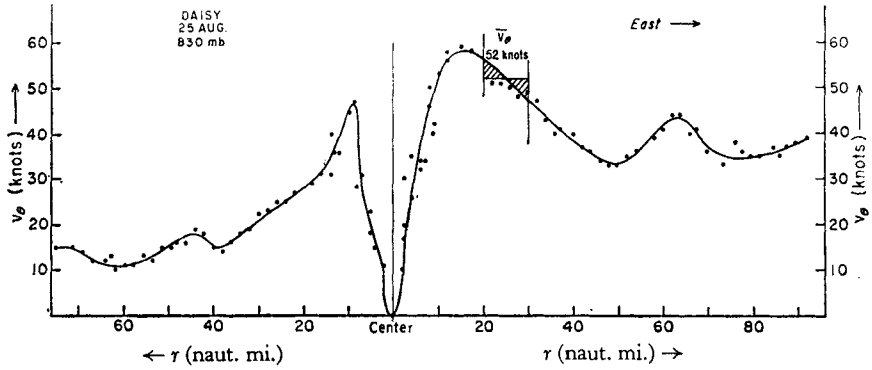


Figure 7. Profile of tengential wind ($v_\theta$) on a W-E traverse through the centre of *Daisy*, 25 August, 830 mb.

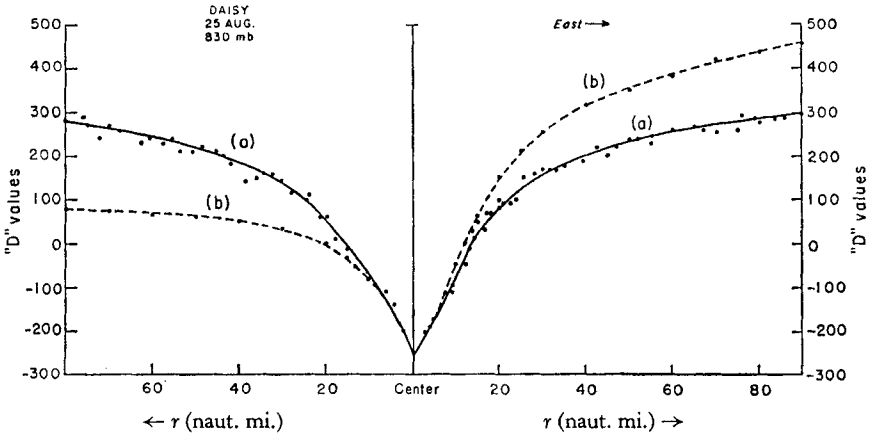


Figure 8. W-E, *D*-value profile through the centre of *Daisy* that goes with the $v_\theta$ profile in Figure 7.
Curve (a) = Actual *D* profile. Curve (b) = Computed *D* profile (i.e., $D_{gr}$).

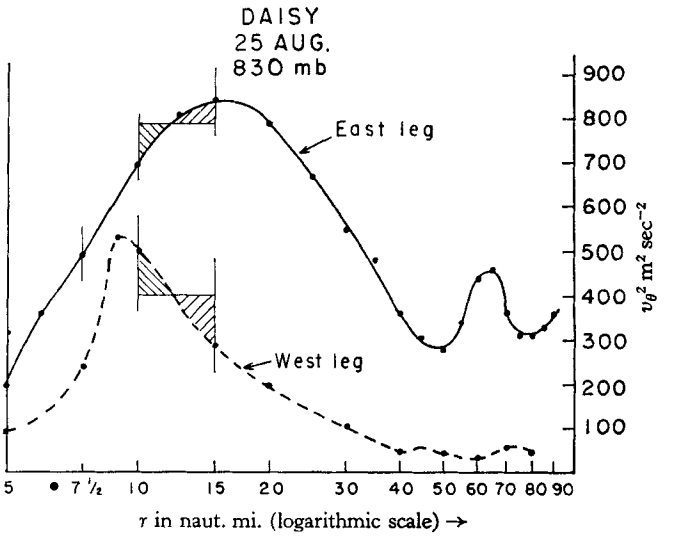


Figure 9. Comparison of $v_\theta^2$ (m$^2$ sec$^{-2}$) profiles along the east and west legs of the traverse through *Daisy* on 25 August, 830 mb. Values of $v_\theta^2$ are plotted against ln r.

Integration of the centrifugal acceleration is given by $\int_{r_1}^{r_2} v_\theta^2/r\, dr = \overline{v_\theta^2} \ln r_2/r_1$, where $\overline{v_\theta^2}$ is the mean value of $v_\theta^2$ between $\ln r_1$ and $\ln r_2$. This quantity is obtained by plotting $v_\theta^2$ vs. $\ln r$ and taking mean values between chosen intervals of $\ln r$. Fig. 9 illustrates the method for graphical determination of $\overline{v_\theta^2}$ between the 10 and 15 naut. mi. radius.

The Coriolis acceleration is obtained by solving $\int_{r_1}^{r_2} f v_\theta\, dr = f\overline{v_\theta}\,(r_2 - r_1)$, where $\overline{v_\theta}$ is the mean of $v_\theta$ between $r_2$ and $r_1$ and $f$ is considered constant. Graphical determination of $\overline{v_\theta}$ is illustrated in Fig. 7.

The value of $f$ at the location of the storm centre was used for each computation period. The greatest latitudinal extent of the computations was only $2\frac{1}{2}°$ latitude. This is equivalent to a maximum variation of $f$ at 25° of only 9 per cent. Since the magnitude of the Coriolis acceleration was usually much less than that of the centrifugal term, especially at high wind speeds near the centre where $f\bar{v}_\theta$ was less than 5 per cent of $\overline{v_\theta^2}/r$, the error in assuming $f$ constant over the whole storm area is negligible. Therefore it was permissible to use a single value for each flight.

We may define

$$g\,(D_2 - D_1)_{\mathrm{gr}} = \overline{v_\theta^2} \ln \frac{r_2}{r_1} + f\bar{v}_\theta\,(r_2 - r_1) \quad . \quad . \quad . \quad (6)$$

where the subscript ' gr ' denotes the $D$-difference which the airplane should have observed with the wind field present (i.e., in the case of $\dot{v}_r)_{\mathrm{gr}} = 0$). This result may be compared with the observed or actual $D$-value gradient denoted by the subscript ' act.' We shall define

$$g\,(D_2 - D_1)' = g\,(D_2 - D_1)_{\mathrm{gr}} - g\,(D_2 - D_1)_{\mathrm{act}} \quad . \quad . \quad (7)$$

where the prime denotes the ' unbalanced ' portion of the $D$-difference. Then

$$\int_{r_1}^{r_2} \dot{v}_r)_{\mathrm{gr}}\, dr = +\,g\,(D_2 - D_1)', \quad \text{or} \quad \dot{v}_r)_{\mathrm{gr}} = +\,g\,\frac{(D_2 - D_1)'}{r_2 - r_1} . \quad . \quad (8)$$

The computations corresponding to the radial traverse along the eastern leg of *Daisy* on 25 August at 830 mb are shown in Table 2. Increments of $r_2 - r_1$ were taken as 5 or 10 naut. mi. from 5 to 20 naut. mi. radius, and as 10 naut. mi. farther out. The largest radius to which computations could be carried was 60 to 80 naut. mi. in most cases. These distances are quite sufficient for a description of the acceleration field in the outer storm areas. Inside the 10 naut. mi. radius, computations could not usually be made owing to uncertainties of centre location. Results in the interval from 10 to 15 miles are, at times, questionable for the same reason.

Along the flight-leg illustrated in Table 2, the gradient along $r$ of $D_{\mathrm{gr}}$ exceeded that of $D_{\mathrm{act}}$ along $r$, so that $\bar{\dot{v}}_r)_{\mathrm{gr}}$ was positive and directed outward. Profiles of both $D_{\mathrm{gr}}$ and $D_{\mathrm{act}}$ are shown in Fig. 8 for the whole traverse from west to east side of *Daisy* on 25 August. Note that whilst the slope of the $D_{\mathrm{gr}}$ profile was greater than that of $D_{\mathrm{act}}$ in the east, the reverse was true in the west. The accumulated differences are substantial – about one-third of the total $D$-drop. Up to this point, the procedure has been nearly rigorous. Finally a more qualitative step was taken.

Computed values of $\bar{\dot{v}}_r)_{\mathrm{gr}}$ for each radial interval did not always yield smooth radial curves. This was caused partly by the integration intervals (i.e., only 5 to 10 naut. mi.) but primarily it was due to the limit of accuracy to which the gradient of $D$ could be measured. Whereas the winds are integrated over the radial interval of $r_1$ to $r_2$, the $D_2 - D_1$ values are obtained by reading off values at individual radii $r_2$ and $r_1$. The original readings (by eye) of radio and pressure altimeters from films of the photopanel*

* The altimeters were not included in the automatic data punching system.

TABLE 2. COMPUTATIONS OF $\dot{v}_r)_{gr}$ ALONG EASTERN RADIAL LEG OF HURRICANE *Daisy* 25 AUGUST AT 830 mb

| radius (naut. mi.) | $\ln \frac{r_2}{r_1}$ | $\overline{v_\theta^2}$ ($10^2$ m$^2$/sec$^2$) | $\frac{1}{g}\overline{v_\theta^2} \ln \frac{r_2}{r_1}$ (ft) | $\overline{v_\theta}$ (m sec$^{-1}$) | $\int \frac{f}{g} dr$ (ft) | $\overline{v_\theta} \int \frac{f}{g} dr$ (ft) | Total (ft) $\frac{1}{g}\overline{v_\theta^2} \ln \frac{r_2}{r_1} + \overline{v_\theta} \int \frac{f}{g} dr$ | Computed $D$ profile (ft) | Observed $D$ profile (ft) | Computed minus observed $D$ profile (ft) | Gradient of $D$ profile difference (ft) | Conversion factor for kt hr$^{-1}$ | $\dot{v}_r)_{gr}$ (kt hr$^{-1}$) | $\dot{v}_r)_{gr}$ with $dr$ increased (kt hr$^{-1}$) |
|---|---|---|---|---|---|---|---|---|---|---|---|---|---|---|
| 5 | | | | | | | | − 170 | − 170 | 0 | | | | |
| | 0·693 | 4·9 | 111 | 22 | 0·2 | 4 | 115 | | | | + 25 | 2·36 | + 59 | + 39 |
| 10 | | | | | | | | − 55 | − 80 | + 25 | | | | |
| | 0·405 | 8·1 | 107 | 28·5 | 0·2 | 6 | 113 | | | | + 8 | 2·36 | + 19 | + 44 |
| 15 | | | | | | | | + 58 | + 25 | + 33 | | | | |
| | 0·288 | 8·1 | 77 | 29 | 0·2 | 6 | 83 | | | | + 23 | 2·36 | + 55 | + 31 |
| 20 | | | | | | | | + 141 | + 85 | + 56 | | | | |
| | 0·405 | 6·6 | 88 | 26 | 0·4 | 10 | 98 | | | | + 26 | 1·18 | + 31 | + 32 |
| 30 | | | | | | | | + 239 | + 155 | + 84 | | | | |
| | 0·288 | 4·5 | 42 | 21·5 | 0·4 | 8 | 50 | | | | + 5 | 1·18 | + 8 | + 13 |
| 40 | | | | | | | | + 289 | + 200 | + 89 | | | | |
| | 0·223 | 3·3 | 24 | 17·5 | 0·4 | 7 | 31 | | | | + 1 | 1·18 | + 1 | + 4 |
| 50 | | | | | | | | + 320 | + 230 | − 190 | | | | |
| | 0·182 | 3·5 | 21 | 18·5 | 0·4 | 7 | 28 | | | | + 3 | 1·18 | + 4 | + 7 |
| 60 | | | | | | | | + 348 | + 255 | + 93 | | | | |
| | 0·154 | 3·9 | 20 | 20·5 | 0·4 | 8 | 28 | | | | + 13 | 1·18 | + 15 | + 7 |
| 70 | | | | | | | | + 376 | 270 | + 106 | | | | |
| | 0·134 | 3·4 | 15 | 17·5 | 0·4 | 7 | 22 | | | | + 2 | 1·18 | + 2 | + 9 |
| 80 | | | | | | | | + 398 | 290 | − 108 | | | | |

*D*-values are given in feet as in the original data. Accelerations are expressed in kt hr$^{-1}$. They have not been converted to cgs units because it was felt that 1 kt hr$^{-1}$ imparts a feeling for the physical magnitudes involved more readily to most readers than $1{\cdot}4 \times 10^{-2}$ cm sec$^{-2}$, its cgs equivalent.

cannot be considered to be more accurate than $\pm$ 10 ft, so that the observed $D$ differences over small radial intervals cannot be regarded as exact, even when read from curves of best fit. In order to overcome this difficulty it was often necessary to increase the radial interval of integration to double or treble those chosen originally, especially at the inner radii, where trebling will increase the radial interval from 5 to 15 naut. mi. This step, although possibly eliminating microscale features, does not obscure hurricane-scale features.

Values of $\overline{v_r})_{gr}$ were plotted on maps at the mid-point of each radial interval $r_2 - r_1$, and isolines were drawn for selected values. A grid was then placed over the analysed $\overline{v})_{gr}$ field in order to obtain averages around the storm at different radii. This averaging yields mean radial profiles of $\overline{v_r})_{gr}$. It should be noted that interpolation by qualitative chart analysis was left to the very end and that all results not depending on this step are free from the subjectivity of line drawing.

Henceforth in this paper the symbol $\overline{v_r})_{gr}$ (i.e., the mean value of $v_r)_{gr}$ between the radial intervals $r_2 - r_1$) will be denoted just by the symbol $v_r)_{gr}$ where the bar above $v_r)_{gr}$ has been deleted. Only when averaging is performed around the storm at selected radii will the bar over $v_r)_{gr}$ be included to denote circular averaging.

Nearly all computations performed and conclusions drawn in this paper are based on data obtained from the 10 levels listed in Table 3. These levels were the ten best covered by National Hurricane Research Project aircraft during the 1956 through 1958 seasons – where reliable wind and $D$-values were obtained.

TABLE 3. DATA OBTAINED FROM TEN LEVELS DURING 1956/1958 SEASONS

| Storm, date and level | Max. wind right quads. (kt) | Max. wind left quads. (kt) | Difference right-left quads. (kt) | Speed of storm × two (kt) | Col. 4/Col. 5 |
|---|---|---|---|---|---|
| *Daisy* 25 August 830 mb | 65 | 35 | 30 | 14 | ≈ 2 |
| *Daisy* 25 August 570 mb | 60 | 45 | 15 | 14 | ≈ 1 |
| *Daisy* 27 August 630 mb | 120 | 85 | 35 | 16 | ≈ 2 |
| *Daisy* 28 August 620 mb | 105 | 55 | 50 | 36 | ≈ 1½ |
| *Cleo* 18 August 820 mb | 90 | 50 | 40 | 28 | ≈ 1½ |
| *Cleo* 18 August 570 mb | 85 | 45 | 40 | 28 | ≈ 1½ |
| *Carrie* 15 August 605 mb | 85 | 50 | 35 | 24 | ≈ 1½ |
| *Carrie* 17 August 690 mb | 95 | 65 | 30 | 26 | ≈ 1½ |
| *Helene* 24 September 635 mb | 60 | 55 | 5 | 20 | ≈ ¼ |
| *Helene* 25 September 810 mb | 80 | 55 | 25 | 12 | ≈ 2 |

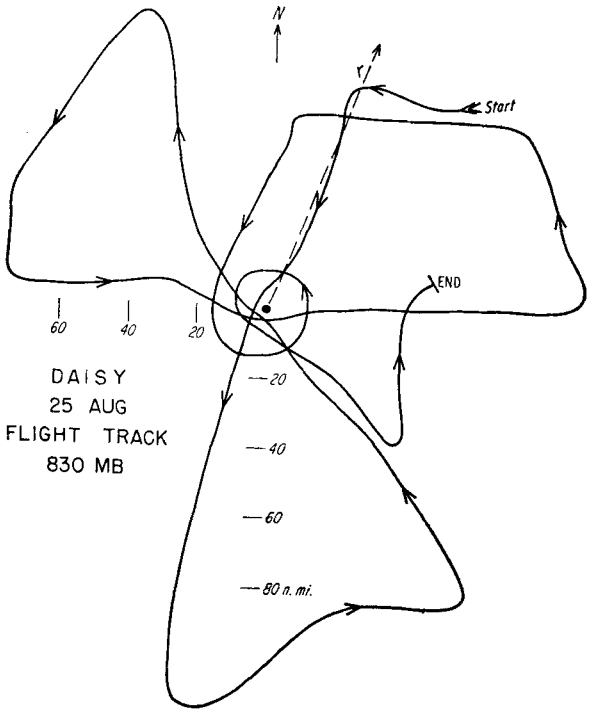


Figure 10. Flight track of hurricane *Daisy*, 25 August, 830 mb.

## 3. Results

### (*1a*) *Radial accelerations – relative to a fixed storm centre*

Calculated values of $\dot{v}_r)_{gr}$ were made along 61 radial legs at the levels listed in Table 1. Figs. 11 and 15 illustrate typical values. All 10 levels have large $\dot{v}_r)_{gr}$ values, which shows that the *radial* gradient wind equation, as here defined, relative to the fixed storm centre (Eq. (3)) does not express the balance of forces *along the radial direction*. In nearly all cases, the areas of strongest winds were places of large positive $\dot{v}_r)_{gr}$ and the areas of weakest winds places of large negative $\dot{v}_r)_{gr}$. Areas of positive $\dot{v}_r)_{gr}$ were usually found in the right quadrants* where the winds were the strongest and negative $\dot{v}_r)_{gr}$ values are found in the left quadrants where the winds were the weakest. With symmetrical pressure distribution around the storm, these would be the proper places for the respective $\dot{v}_r)_{gr}$ accelerations with an asymmetric wind field related, at least in part, to the storm's movement. However, this asymmetry in the wind field can seldom be accounted for by subtracting out the speed of the storm (Table 3).

The order of magnitude of $\dot{v}_r)_{gr}$ was 10 to $10^2$ kt $hr^{-1}$ over most portions of the hurricane with range from zero to approximately 300 kt $hr^{-1}$. The average absolute maximum for all storm levels was between 100 and 200 kt $hr^{-1}$. These magnitudes are a large fraction of the radial pressure gradient or radial Coriolis and centrifugal accelerations. Figs. 14 and 18 contain typical area distributions of the ratio $\dot{v}_r)_{gr}/(f\overline{v_\theta} + \overline{v_\theta^2}/r)$ for two of the pressure levels flown. It was unexpected that $\dot{v}_r)_{gr}$ would be so large a fraction of the centrifugal plus Coriolis accelerations. In many places, especially in the western quadrants, this ratio exceeded unity. There the radial pressure gradient force greatly exceeded the radial centrifugal and Coriolis acceleration.

* The right-front quadrant is the area in the 0° to 90° sector, when the direction of movement of the storm is taken as the zero degree line on a 360° compass, counting clockwise. Other sectors have corresponding relations.

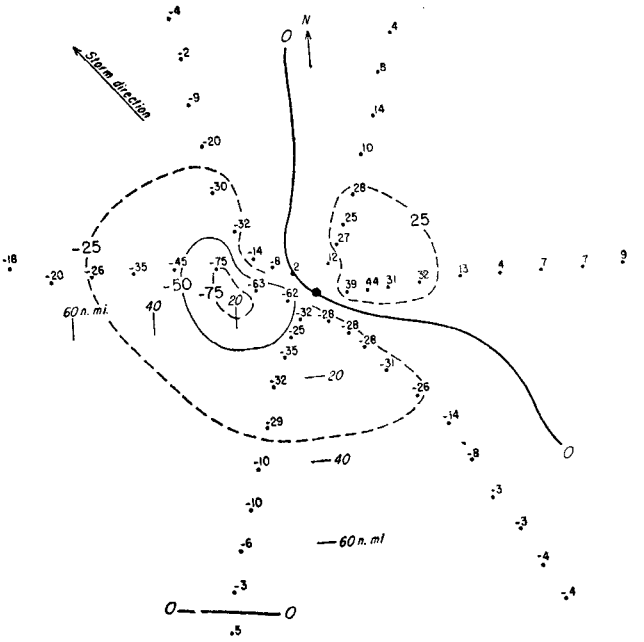


Figure 11. Hurricane *Daisy*, 25 August, 830 mb, $\dot{v}_r)_{gr}$ in kt hr$^{-1}$.

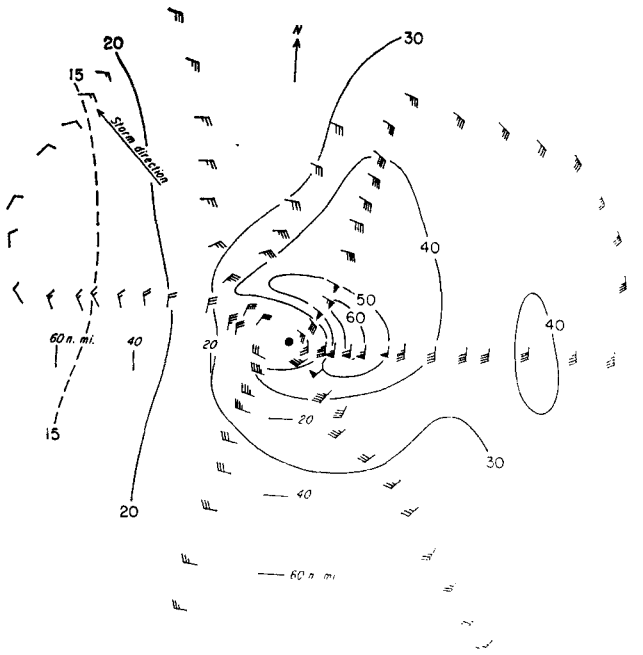


Figure 12. Hurricane *Daisy*, August 25, isotachs (kt).

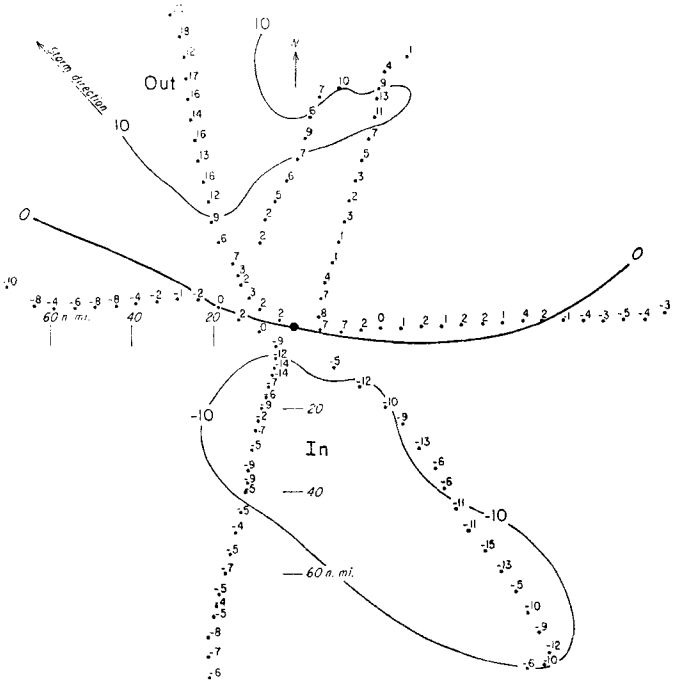


Figure 13. Radial wind component, hurricane *Daisy*, $v_r$ (kt).

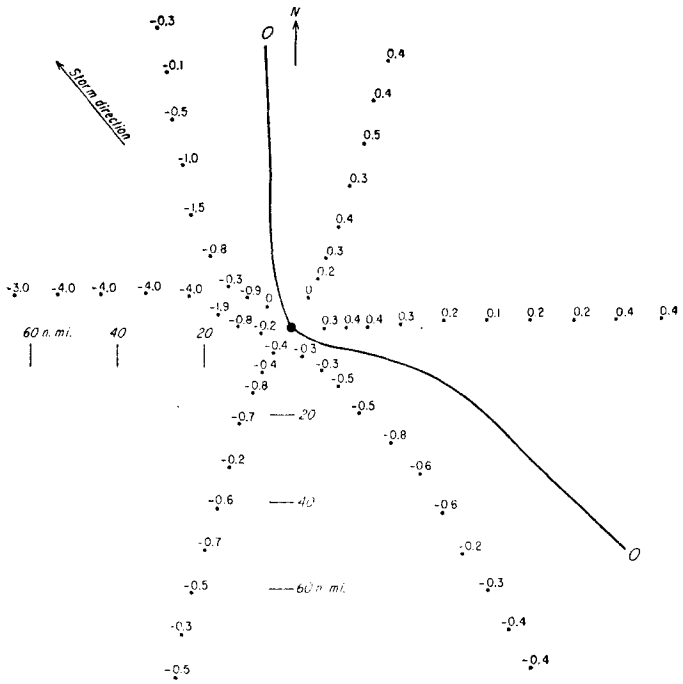


Figure 14. Hurricane *Daisy*, $\dfrac{\dot{v}_r)_{gr}}{f\bar{v}_\theta + \dfrac{\overline{v_\theta^2}}{r}}$

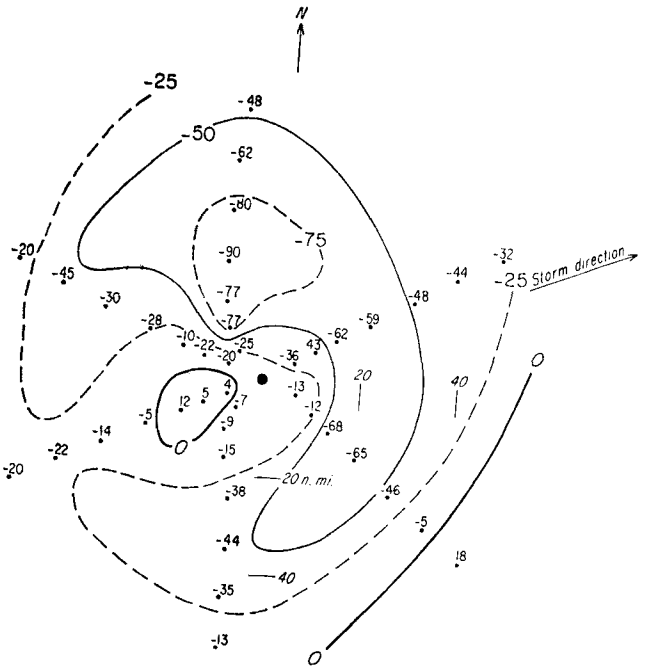


Figure 15. Hurricane *Carrie*, 17 September, 690 mb, $\dot{v}_T)_{gr}$ in kt hr$^{-1}$.

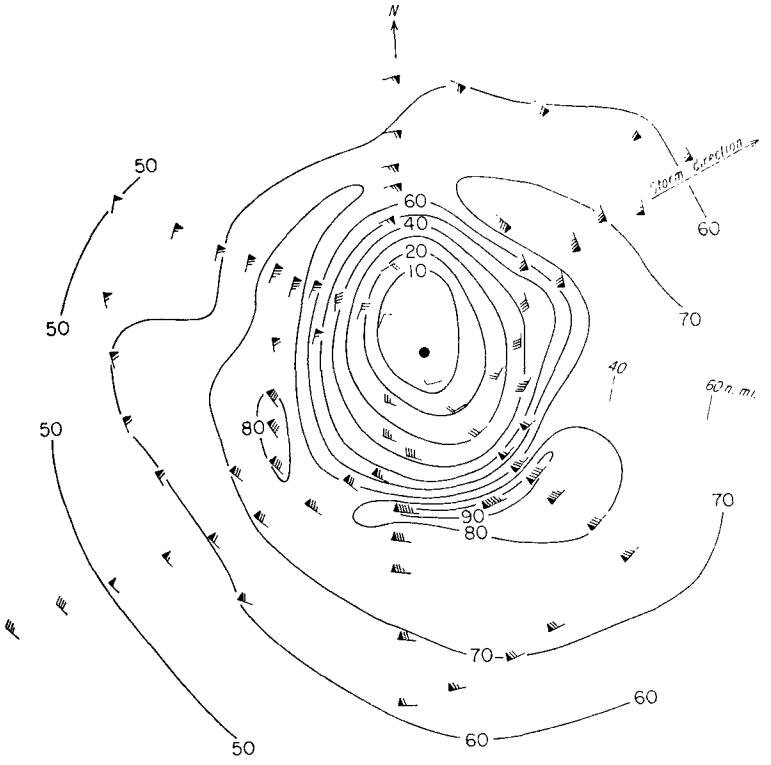


Figure 16. Hurricane *Carrie*, 17 September, 690 mb, isotachs (kt).

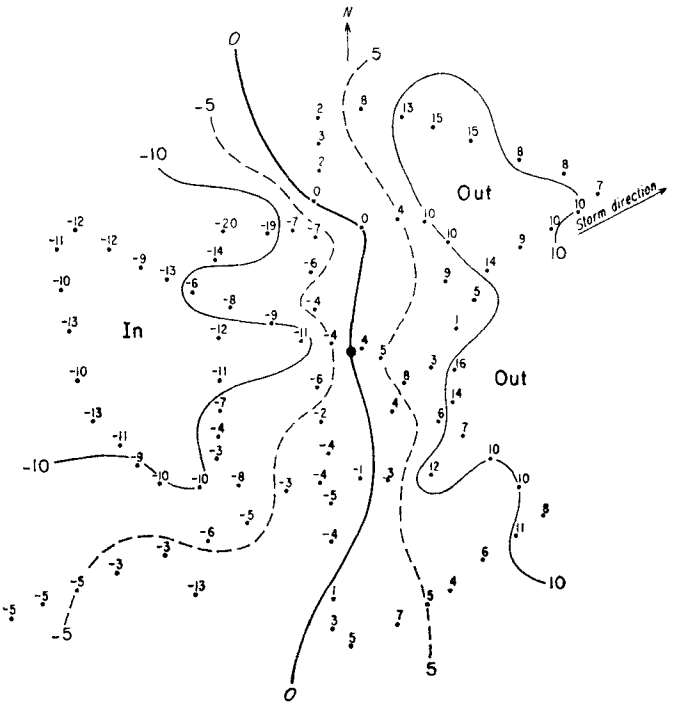


Figure 17. Radial wind component, hurricane *Carrie*, 17 September, 690 mb, $v_r$ (kt).

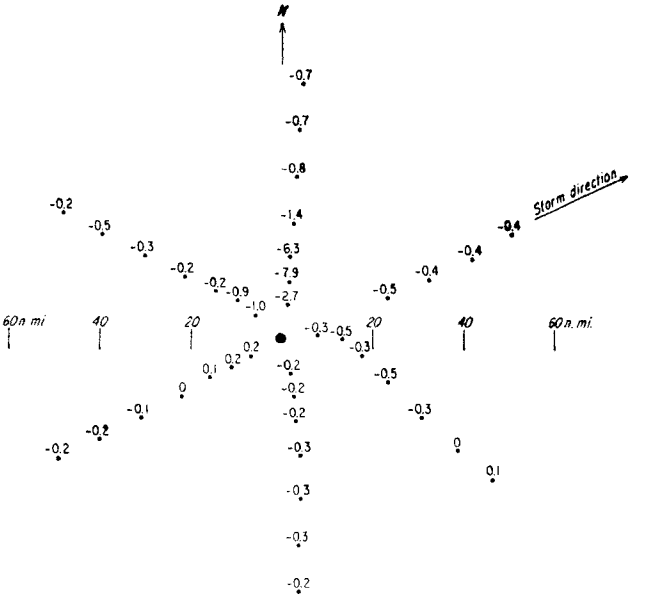


Figure 18. Hurricane *Carrie*, 17 September, 690 mb, $\dfrac{\dot{v}_r)_{gr}}{fv_\theta + \dfrac{v_\theta^2}{r}}$

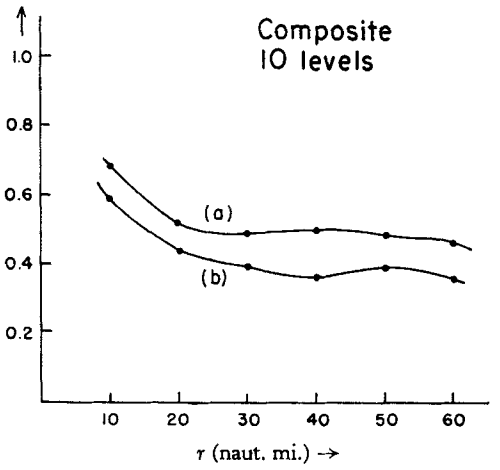


Figure 19. (a) $\frac{\overline{\dot{v}_r)_{gr}}}{f\overline{v}_\theta + \frac{\overline{v}_\theta^2}{r}}$ (b) $\frac{\overline{\dot{v}_r)_{gr}}}{\frac{\overline{\partial D}}{\partial r}}$

Values are plotted against radius after averaging round the storm without respect to the sign $\dot{v}_r)_{gr}$.

Fig. 19 contains a radial composite of $\overline{\dot{v}_r)_{gr}}/(f\overline{v_\theta} + \overline{v_\theta^2}/r)$ for all 10 flights. There $\dot{v}_r)_{gr}$ averages between 50 and 60 per cent of the radial centrifugal and Coriolis accelerations. A similar composite of the integrated radial profile of $\overline{\dot{v}_r)_{gr}}/\overline{g\,\partial D/\partial r}$ shows that $\dot{v}_r)_{gr}$ averages 40 to 50 per cent of the radial pressure-gradient force. The difference between these two composites is due to the fact that the radial pressure force averaged 10 to 15 per cent more than the radial Coriolis and centrifugal accelerations (to be discussed later). Fig. 24 is a 10-level composite of the absolute values of $\overline{\dot{v}_r)_{gr}}$, $\overline{g\,\partial D/\partial r}$, and $(f\overline{v}_\theta + \overline{v_\theta^2}/r)$ plotted against radius. An area composite of $\dot{v}_r)_{gr}$, both with and without respect to sign is shown in Figs. 20 and 21. The area composite with respect to sign clearly shows the asymmetry of $\dot{v}_r)_{gr}$ between right and left quadrants of the storm. All area compositing has been done with respect to the direction of motion of the storms.

### (*Ib*) *Radial accelerations – relative to the moving storm centre* $(\dot{v}_{rr})_{gr}$)*

The above results have shown the radial accelerations relative to the instantaneous *fixed point* of the storm's centre. Accelerations relative to the *moving storm centre* will now be considered.

By assuming that the storm moves at constant speed and direction, one can obtain these radial accelerations within the limits of accuracy of the data by subtracting the tangential component of the storm motion ($c_\theta$) from the total tangential wind component in Eq. (5)†. Other terms which arise from this change of reference to the moving storm centre are less than 5 kt $hr^{-1}$ and can be disregarded. This is over an order of magnitude lower than most of the computed $\dot{v}_{rr})_{gr}$ values. The acceleration of the storm displacement also enters into the calculations, but at the times of the calculations the storms were moving at nearly constant direction. Changes in the rate of displacement were also small (less than one or two kt $hr^{-1}$). Thus the acceleration of the hurricane's movement was neglected.

* Any reference to *actual* winds will be with respect to an instantaneously fixed coordinate system. All reference to *relative* winds will refer to winds with the moving centre as reference.

† Rigorous verification of this has been accomplished from the absolute equations of motion in both vector and cartesian form.

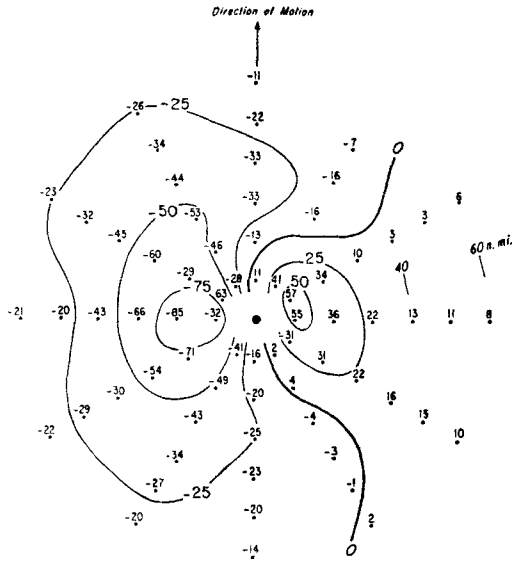


Figure 20. Composite of 10 levels $\dot{v}_r)_{gr}$ in kt hr$^{-1}$, with respect to sign.

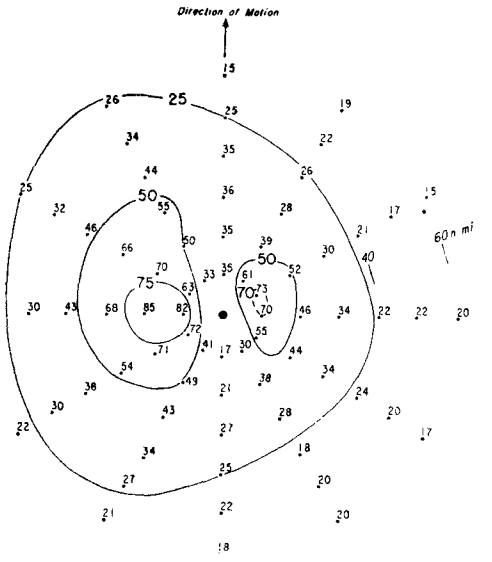


Figure 21. Composite of 10 levels, $\dot{v}_r)_{gr}$ in kt hr$^{-1}$, without respect to sign.

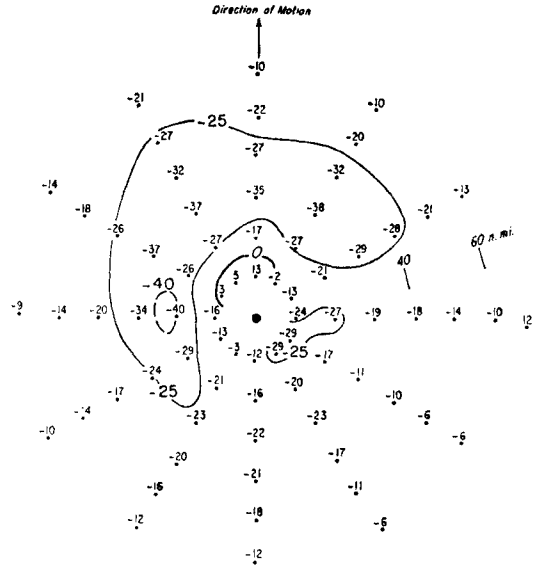


Figure 22. Composite of 10 levels $\dot{v}_{rr})_{gr}$ in kt hr$^{-1}$ with respect to sign.

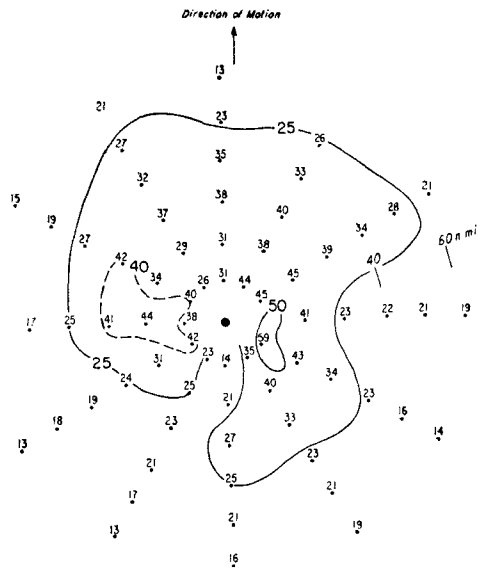


Figure 23. Composite of 10 levels $\dot{v}_{rr})_{gr}$ in kt hr$^{-1}$ without respect to sign.

With these omissions, the equation for the radial acceleration relative to the *moving storm centre*, here denoted by $\dot{v}_{rr})_{gr}$, is

$$\dot{v}_{rr})_{gr} = -g\frac{\partial D}{\partial r} + f(v_\theta - c_\theta) + \frac{(v_\theta - c_\theta)^2}{r}, \quad \text{or}$$

$$\dot{v}_{rr})_{gr} = \left(-g\frac{\partial D}{\partial r} + fv_\theta + \frac{v_\theta^2}{r}\right) - \left(fc_\theta + \frac{2v_\theta c_\theta}{r} - \frac{c_\theta^2}{r}\right) \quad . \quad . \quad (9)$$

where $c_\theta$ is the tangential component of the storm's motion. It is defined positive in the direction of the storm motion. $c_\theta$ is thus positive in the right quadrants and negative

in the left quadrants. Substituting from Eq. (5) we obtain

$$\dot{v}_{rr})_{gr} + \left(fc_\theta + \frac{2v_\theta c_\theta}{r} - \frac{c_\theta^2}{r}\right) = \dot{v}_{r})_{gr}, \quad \text{or}$$

$$\dot{v}_{rr})_{gr} = \dot{v}_{r})_{gr} - M \quad . \quad . \quad . \quad . \quad . \quad . \quad (10)$$

where

$$M = \left(fc_\theta + \frac{2v_\theta c_\theta}{r} - \frac{c_\theta^2}{r}\right) \quad . \quad . \quad . \quad . \quad . \quad (11)$$

The term $fc_\theta$ was always less than 5 kt hr$^{-1}$, and hence had little effect on the calculations. The absolute value of $2v_\theta c_\theta/r$ was usually 4 to 6 times greater than $c_\theta^2/r$. It is then the $2v_\theta c_\theta/r$ term that largely determines the values of $M$. Thus approximately

$$\dot{v}_{rr})_{gr} = \dot{v}_{r})_{gr} - \frac{2v_\theta c_\theta}{r}$$

In general $\dot{v}_{rr})_{gr} < \dot{v}_{r})_{gr}$. In the right quadrants, where $\dot{v}_{r})_{gr}$ is positive, $v_\theta$ and $c_\theta$ are also positive so that this term subtracts from $\dot{v}_{r})_{gr}$. In the left quadrants, with $\dot{v}_{r})_{gr}$ negative, $v_\theta$ positive and $c_\theta$ negative, $\dot{v}_{r})_{gr}$ is also reduced. Since $v_\theta$ is greater in the right than in the left quadrants, the effect of the correction is strongest in the right quadrants. In the front and rear of the hurricane the correction, of course, is not present as $c_\theta$ vanishes.

Values of $M$ were computed and inserted in Eq. (10). The resulting $\dot{v}_{rr})_{gr}$ patterns differed from those of $\dot{v}_{r})_{gr}$ as follows :

(1). The values of $\dot{v}_{rr})_{gr}$ were generally smaller than those of $\dot{v}_{r})_{gr}$, being approximately 60 to 80 per cent of the $\dot{v}_{r})_{gr}$ values.

(2). The positions of many of the $\dot{v}_{rr})_{gr}$ centres were shifted from those of the $\dot{v}_{r})_{gr}$ centres.

(3). Sometimes $M$ exceeded $\dot{v}_{r})_{gr}$ in the right quadrants so that $\dot{v}_{rr})_{gr}$ became negative. In consequence, the area with negative $\dot{v}_{rr})_{gr}$ is very large compared with that of positive $\dot{v}_{rr})_{gr}$ on most of the levels analysed.

Ten-level area composites of $\dot{v}_{rr})_{gr}$ both *with* and *without* respect to sign are shown in Figs. 22 and 23. Again compositing has been done with respect to the direction of motion of each storm. The composite without respect to sign resembles the $\dot{v}_{r})_{gr}$ pattern in the essential features : maximum accelerations to the right and left of the direction of motion, respectively (Fig. 23). This is an important result in that one might have expected the hurricanes to approach circular symmetry once the effect of centre propagation was removed.

It follows that neither the asymmetry nor the radial acceleration field itself is removed by defining the computation with respect to the *moving centre*. Since most flight levels were in the middle troposphere, where the net mass inflow or outflow are small, one might have thought that $\dot{v}_{rr})_{gr}$ should vanish here, especially when integrated around the storm. Such, however, is not the case.

We shall now return to the $\dot{v}_{r})_{gr}$ fields and study their characteristics in relation to other storm features.

### (2). *Relation of the fields of* $\dot{v}_{r})_{gr}$ *to* $v_r$ *and the maximum wind*

Analysis of the fields of the actual radial component of motion at all middle and lower tropospheric levels showed that *in general* there was a line dividing inflow and outflow regions around the hurricane; further that this line usually closely bisected the areas of largest inward directed $\dot{v}_{r})_{gr}$ in the left quadrants and of largest outward directed $\dot{v}_{r})_{gr}$ in the right quadrants (compare Figs. 11 and 13 and Figs. 15 and 17).

In the right and left front quadrants of the storm, $v_r$ itself was predominantly directed outward. Inward directed motion occurred mainly in the rear quadrants. Thus in the

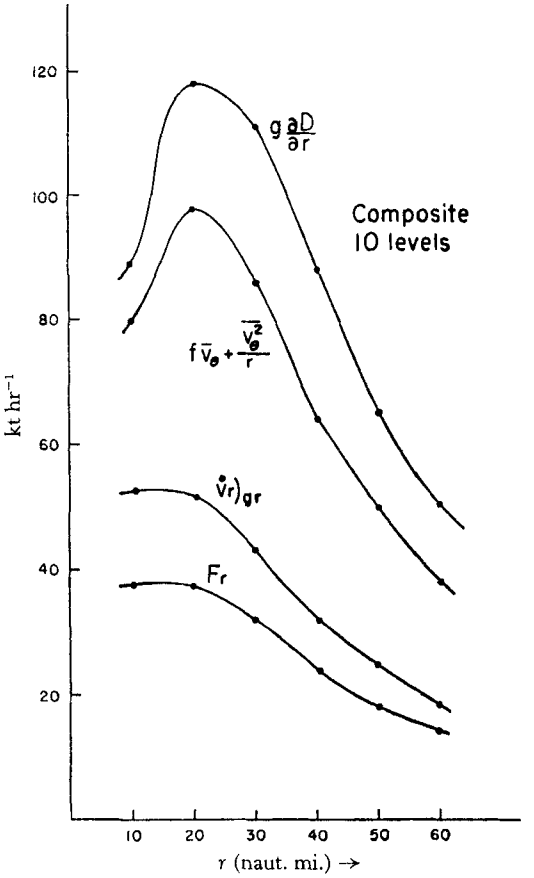


Figure 24. Radial profiles of various accelerations at selected radii. Values have been averaged around storm without respect to sign.

right front quadrant $v_r$ and $\dot{v}_r)_{gr}$ both pointed outward; in the left rear quadrant they both pointed inward. In the right rear quadrant, where the winds had inward radial components, this component decreased and reversed to the downstream side in agreement with the $\dot{v}_r)_{gr}$ field. The reverse was true for the left front quadrant. This observation agrees with findings of a study by Ausman (1959) who, working with surface ship data of many hurricanes, has shown that $v_r$ is directed inward in the rear quadrants and outward in the front quadrants at radii from 2° to 6° latitude from the centre. From the present findings this appears to be valid over the whole hurricane area, not only at these outer radii, but also near the centre.

It is an interesting fact that $v_r$ is zero approximately at the location of the maximum winds; there its sign changes from negative to positive looking downstream. $\dot{v}_r)_{gr}$ is also positive and has maximum values very near this change from negative to positive $v_r$.

Qualitatively, this coincidence may render insight on the production of the maximum winds. In the region of weak winds in the left quadrants, air is accelerated inward and acquires a large crossing angle toward lower pressure. After some time the wind speed increases sufficiently so that gradient balance in the radial direction is established ($\dot{v}_r)_{gr} = 0$). At this point, however, the mass is still crossing towards lower pressure and gaining kinetic energy. It then overshoots the radius of gradient equilibrium and continues toward the centre with $\dot{v}_r)_{gr}$ directed outward. The speed increases until the air moves parallel with the contours of the isobaric surfaces. There the place of strongest winds and also the maximum $\dot{v}_r)_{gr}$ is reached. As the air then turns outward towards higher contours, both wind speed and $\dot{v}_r)_{gr}$ again decrease.

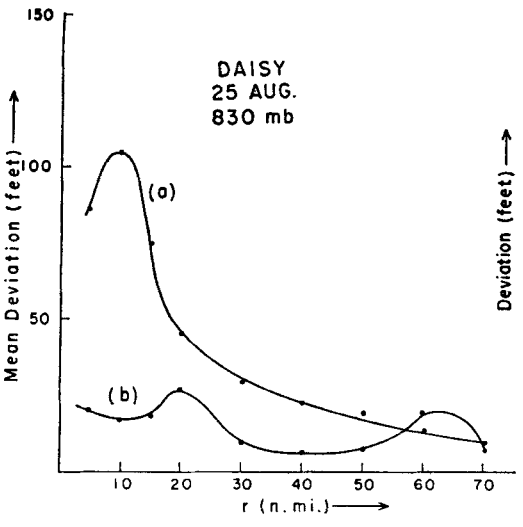


Figure 25. Hurricane *Daisy*, 830 mb, 25 August. Mean deviation of profiles of the individual radial flights legs at selected radii from their mean value (ft).

Curve (a) = $D_{gr}$. Curve (b) = $D_{act}$.

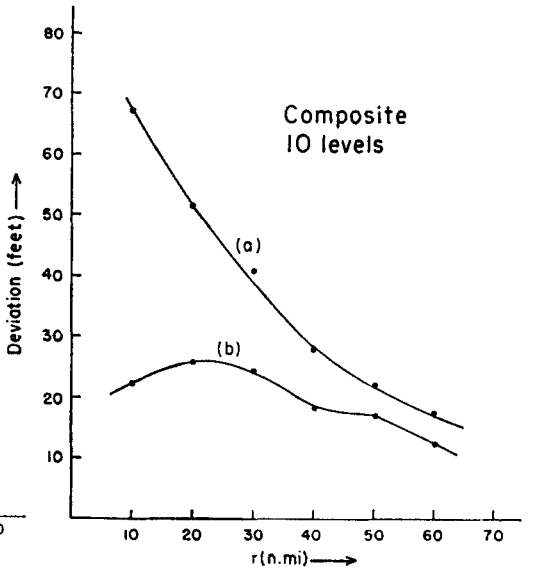


Figure 26. Composite of 10 levels. Mean deviation of profiles of the individual radial flight legs at selected radii from their mean value (ft).

Curve (a) = $D_{gr}$. Curve (b) = $D_{act}$.

### (3). *Comparison of the asymmetries of* $g\,\partial D/\partial r$ *and* $(f\bar{v}_\theta + \overline{v_\theta^2}/r)$ *around the storms*

The question may be asked whether the $\dot{v}_r)_{gr}$ field arises from asymmetries of the pressure gradient force, or of the $(f\bar{v}_\theta + \overline{v_\theta^2}/r)$ distribution around the centre. In order to answer this question, the fields of $D_{act}$ and $D_{gr}$ were drawn on maps. At selected radii, the averages of $D_{act}$ and of $D_{gr}$ were determined. From a grid (Fig. 6) spaced evenly at 30° intervals, the mean deviation from the average around the centre was computed at each of the chosen radii.

Figure 25 is a typical example. Curves (a) show the deviation of $D_{gr}$ (i.e., the wind field), and curves (b) the deviation of $D_{act}$ (i.e., the pressure field). Though the curves on the different days vary considerably, certain features nevertheless stand out. At all levels, except *Helene* 24 September 635 mb, the mean deviation of $D_{act}$ never exceeded that of $D_{gr}$. Hence, asymmetry of the *wind field* in 9 of the 10 cases was then greater than that of the *pressure field*. This feature was especially prominent on three of the *Daisy* flights and in *Cleo* at 820 mb. This result does not obviously follow from the common knowledge that winds are stronger to the right than to the left of the direction of motion. One might have thought that the $D_{gr}$ field would vary concomitantly with $D_{act}$. A radial composite for all 10 levels is seen in Fig. 26. The deviation of the pressure field varies little with radius, while the $D_{gr}$ deviations increase greatly towards the storm centre. In the core of maximum winds the deviation of $D_{gr}$ exceeds that of $D_{act}$ by a factor of three. Symmetry in the pressure field is produced as the heat released in ascending towers is swept around the centre by the strong winds; and the $\dot{v}_r)_{gr}$ field is related more closely to variations of the tangential wind around the storm than to variations of the pressure gradient.

### (4). *Further analysis of* $\dot{v}_r)_{gr}$ *field in stationary coordinates*

As the actual radial wind component is rarely observed to exceed 25 kt, and as individual air parcels often blow through areas of $\dot{v}_r)_{gr}$ of 50 to 100 kt hr$^{-1}$ for 30 to 60 min, it follows qualitatively that $\dot{v}_r \neq \dot{v}_r)_{gr}$, at least over large portions of a hurricane. This

interesting observation will now be analysed by an attempt to compute $\dot{v}_r$ directly. In Eulerian coordinates

$$\dot{v}_r = \frac{\partial v_r}{\partial t} + v_\theta \frac{\partial v_r}{r\,\partial \theta} + v_r \frac{\partial v_r}{\partial r} + w \frac{\partial v_r}{\partial z} \quad . \quad . \quad . \quad (12)$$

Only the term $v_r\,\partial v_r/\partial r$ can be evaluated directly from the flight data; the range of magnitude was 1 to 10 kt hr$^{-1}$ after integration over 10 naut. mi. radial legs. Most values were less than 5 kt hr$^{-1}$ however. The vertical advection term cannot be computed at all, but from general knowledge of vertical motion and vertical wind shear fields the order of magnitude should not exceed that of the radial advection, again after integration over 10 naut. mi. radial distances. The $w\,\partial v_r/\partial z$ term was thus neglected. For computing the tangential advection reliable $v_\theta$ fields are available through analysis; the weak link is $\partial v_r/r\partial\theta$ which was obtained by tabulating the analysis of $v_r$ prescribed in this paper on the grid of Fig. 6. In spite of the weakness of the computation, systematic features of the tangential advection were obtained and reliable features should be revealed by the ten cases. The calculated magnitude of this term had the order of 10 kt hr$^{-1}$ with range from 0 to 50 kt hr$^{-1}$.

The quantity $\partial v_r/\partial t$ was determined by moving the $v_r$-field across the fixed grid of Fig. 6 with the direction and speed of the storm motion. For the fast-moving storms changes were computed from one-half hour before to one-half hour after the time when the $v_r$-field centre position was connected with the fixed grid centre. For slower moving systems the time interval chosen for $\partial/\partial t$ was from one hour before to one hour after the time when the centre position corresponded with the fixed grid centre.

Initial expectation was that $\dot{v}_r)_{gr} = \partial v_r/\partial t + v_\theta\,\partial v_r/r\,\partial\theta + v_r\,\partial v_r/\partial r$ within computational limits. This proved not to be correct by wide margins. The *Daisy* flight of 27 August at 630 mb provides a typical illustration. Fig. 28 contains the field of $\dot{v}_r$, to be compared with Fig. 27. Only 40-60 per cent of the $\dot{v}_r)_{gr}$ field is accounted for by $\dot{v}_r$. Broadly speaking, the orientation of the patterns and centre locations are in fair agreement. Fig. 29 contains the difference field. From the earlier definition

$$F_r = \dot{v}_r - \dot{v}_r)_{gr} \quad . \quad . \quad . \quad . \quad (13)$$

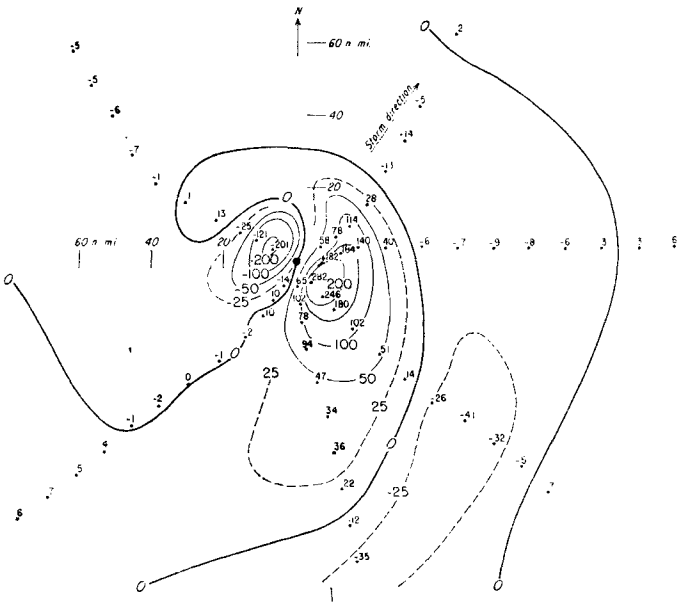


Figure 27. Hurricane *Daisy*, 27 August, 630 mb, $\dot{v}_r)_{gr}$ (kt hr$^{-1}$).

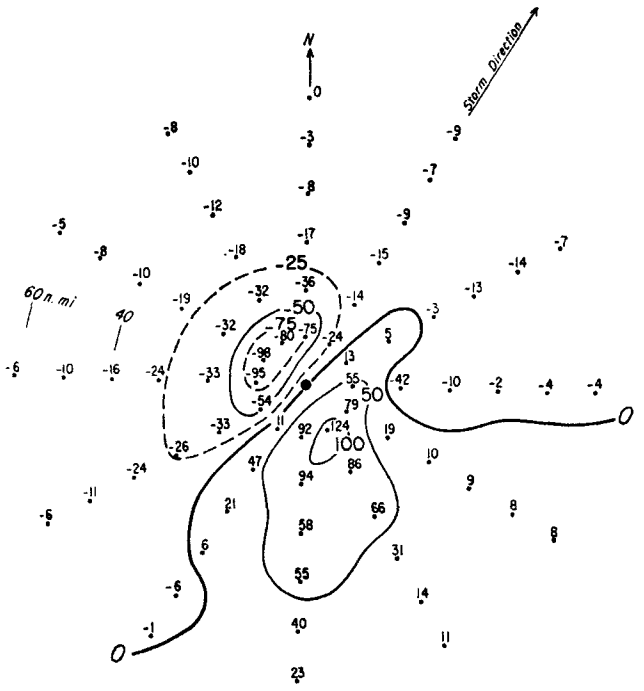


Figure 28. Hurricane *Daisy*, 27 August, 630 mb, $\dot{v}_T$ (kt hr$^{-1}$).

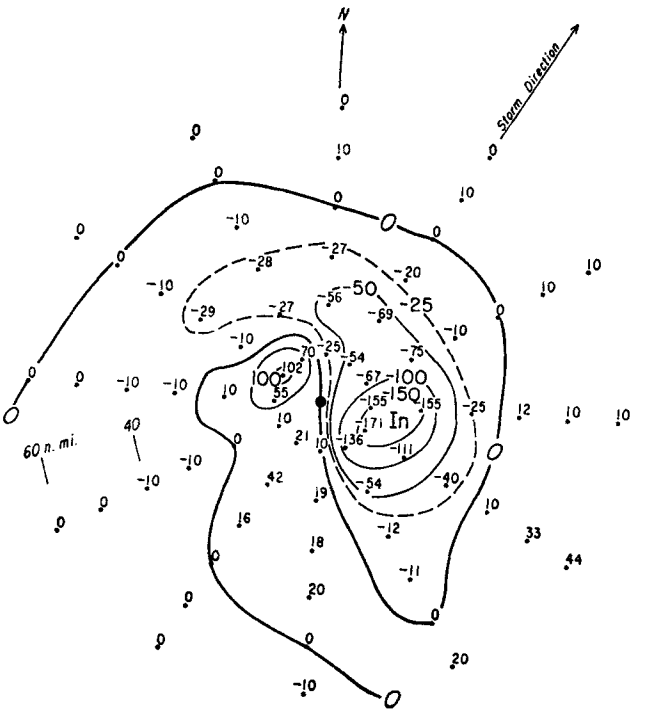


Figure 29. Hurricane *Daisy*, 27 August, 630 mb, $F_T$ (kt hr$^{-1}$), computed frictional force.

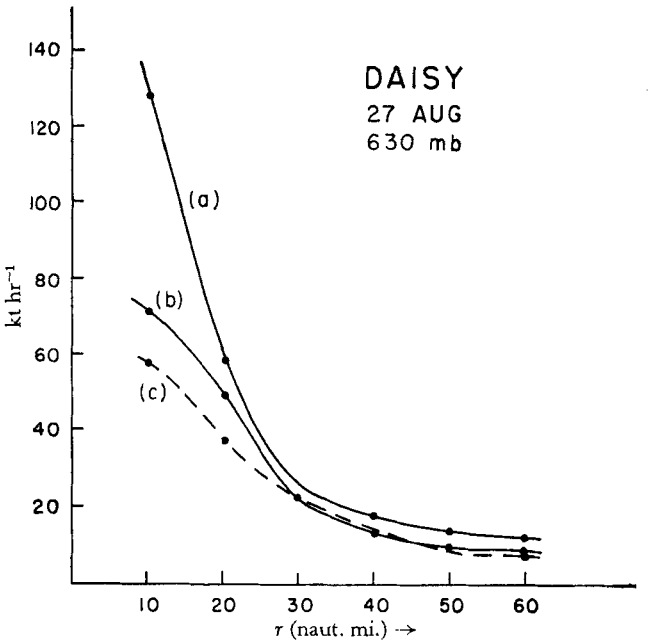


Figure 30. Hurricane *Daisy*, 27 August, 630 mb, averaged around storm without respect to sign (units kt $hr^{-1}$).
Curve (a) = $\dot{v}_r)_{gr}$ Curve (b) = $F_r$ Curve (c) = $\dot{v}_r$

it must now be postulated that Fig. 29 represents the $F_r$ field after subtraction of Fig. 27 from Fig. 28 in the sense of Eq. 13. Admittedly this postulated force field is exceedingly strong (0·1 to 3 dynes/unit mass). But in a strongly turbulent system such as the hurricane, the existence of such strong frictional forces should not be rejected *a priori*. Further comments on the magnitude of $F_r$ will be offered shortly.

Fig. 30 contains radial profiles of $\dot{v}_r)_{gr}$, $F_r$, and $\dot{v}_r$ averaged around the storm at 10 naut. mi. intervals for *Daisy* 27 August, 630 mb. We see that $F_r$ and $\dot{v}_r$ are nearly equal

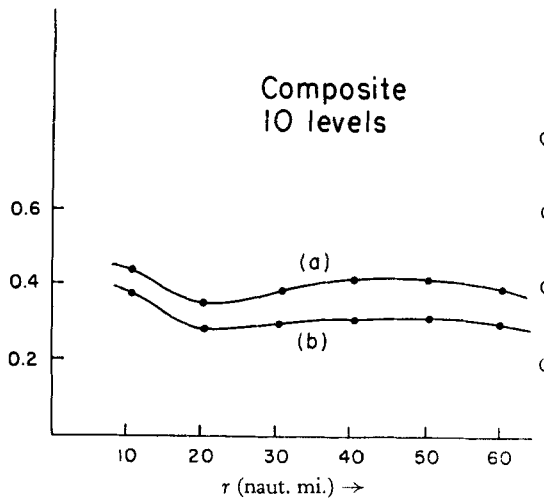


Figure 31. Composite of 10 levels averaged around storm, without respect to sign

Curve (a) $\dfrac{\bar{F}_r}{f \cdot \bar{v}_\theta + \dfrac{\overline{v_\theta^2}}{r}}$ Curve (b) $\dfrac{\bar{F}_r}{g \dfrac{\partial \bar{D}}{\partial r}}$

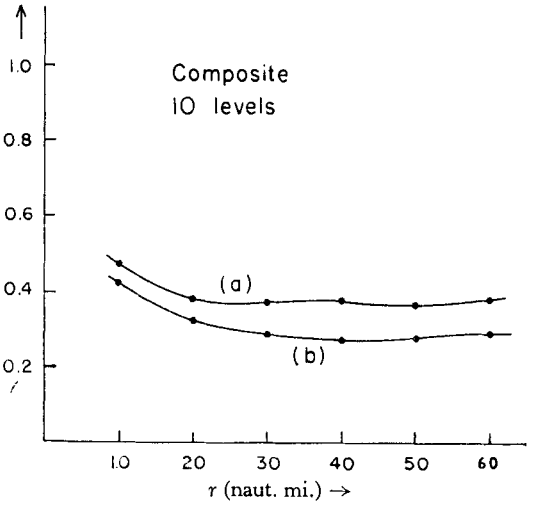


Figure 32. Composite of 10 levels averaged around storm, without respect to sign

Curve (a) $\dfrac{\dot{v}_r}{f \cdot \bar{v}_\theta + \dfrac{\overline{v_\theta^2}}{r}}$ Curve (b) $\dfrac{\dot{v}_r}{g \dfrac{\partial \bar{D}}{\partial r}}$

and average over half the $\dot{v}_r)_{gr}$ values. That $|F_r + \dot{v}_r| > |\dot{v}_r)_{gr}|$ at all radii is due to the lack of exact superpositioning of $\dot{v}_r)_{gr}$ and $\dot{v}_r$ centres.

Similar properties were obtained for the other hurricanes so that it was considered permissible to form the average of all ten cases, Figs. 24, 31 and 32. Here also, $F_r$ and $\dot{v}_r$ are nearly equal. $F_r$ approaches 85 per cent of $\dot{v}_r)_{gr}$ at radii from 30 to 60 naut. mi., and 70 per cent over the whole radial distance. Since $\dot{v}_r)_{gr}$ itself was a large fraction of $g\,\partial D/\partial r$, it follows that the radial frictional and pressure gradient forces have roughly the same magnitude, at least over substantial portions of a hurricane.

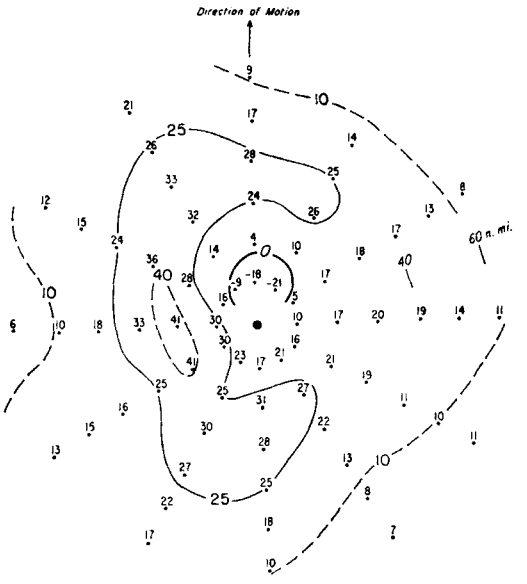


Figure 33. Composite of 10 levels, with respect to sign, $F_r$ or $F_{rr}$ (kt hr$^{-1}$).

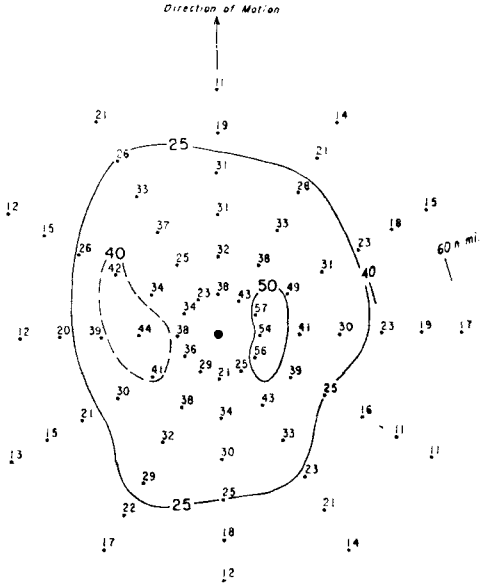


Figure 34. Composite of 10 levels, without respect to sign, $F_r$ or $F_{rr}$ (kt hr$^{-1}$).

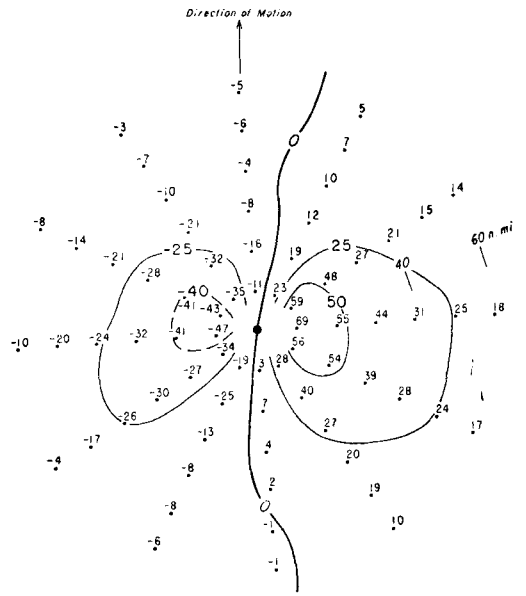


Figure 35. Composite of 10 levels, with respect to sign $\dot{v}_r$ (kt hr$^{-1}$).

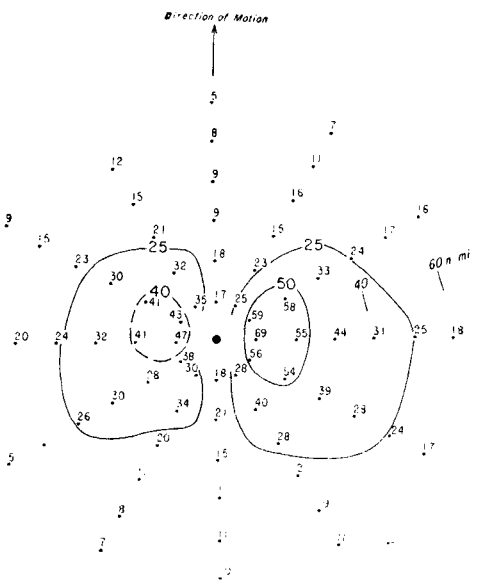


Figure 36. Composite of 10 levels, without respect to sign $\dot{v}_r$ (kt hr$^{-1}$).

In one respect, *Daisy* 27 August, 630 mb was not typical, namely that it was the only level studied with net positive $\dot{v}_r)_{gr}$ values after integration around the centre. The balancing frictional force had to be directed inward. *Daisy* on the 27 August had reached maximum intensity; its winds were slightly stronger than the pressure gradient and $\dot{v}_r)_{gr}$ was directed outward. The storm was just beginning to fill at this time. In eight of the other nine cases, the pressure gradient force exceeded the centrifugal plus Coriolis acceleration – in the integral around the hurricanes. The net $\dot{v}_r)_{gr}$ field consequently was directed inward and $F_r$ outward in these cases.

Figs. 33 and 34 portray 10 level area composites with respect to storm direction of $F_r$ *with* and *without* respect to sign. Fig. 33 illustrates the predominance of outward directed $F_r$ especially well. Figs. 35 and 36 portray 10-level area composites of $\dot{v}_r$ both *with* and *without* respect to sign. It is clearly evident that the values of $\dot{v}_r$ are not of great enough magnitude to account for the $\dot{v}_r)_{gr}$ accelerations even when individual storm level superpositioning of these two fields is eliminated by the 10-level average.

The above calculations have determined the $F_r$ accelerations relative to an instantaneous *fixed point* of the storm centre. The frictional acceleration with respect to the *moving* storm centre (denoted $F_{rr}$) is identical with that with respect to the instantaneous *fixed* centre when the storm propagation is assumed constant.*

The existence of an imbalance in the *cylindrical* gradient wind equation also implies an imbalance of the gradient wind equation in *natural* coordinates.

### (5). *Preliminary comments on the magnitude of* $F_r$

From the discussions of Reynolds (1895) it appears possible to represent $F_r$ by the Reynolds form of eddy stresses. In cylindrical coordinates, $F_r$ then has four components,

$$\frac{\partial}{r\,\partial\theta}\widetilde{v_\theta' v_r'}, \quad \widetilde{\frac{\partial}{r\,\partial r} r\,\bar{v}_r'^2}, \quad \frac{\partial}{\partial z}\widetilde{v_r' w'}, \quad \widetilde{\frac{v_\theta'^2}{r}}$$

where the wavy bar denotes area average and the prime represents deviations from this mean. In this form the term $\partial/\partial z\,\widetilde{v_r' w'}$ would be the vertical gradient of the horizontally integrated product of the radial and vertical wind eddies.

Evaluations of $v_r'$ and $v_\theta'$ values and their tangential and horizontal gradients was made on a number of the mid-tropospheric levels here studied from the Doppler winds, Indicated Airspeed meters and from continuous pitot tube recordings mounted on the aircraft.

From the preliminary computations $\widetilde{\partial/r\,\partial\theta\, v_\theta' v_r'}$, $\widetilde{\partial/r\,\partial r\, r v_r'^2}$ and $\widetilde{v_\theta'^2/r}$ turn out to be quite small and cannot account for $F_r$. An order of magnitude estimate of the $\partial/\partial z\,\widetilde{v_r' w'}$ term, using determined values of $v_r'$ from the Doppler winds, Indicated Airspeed meters and pitot tubes, and assuming Malkus (1959) and Riehl's (1960)† calculations of vertical velocities in hurricane Cb's, indicates that this term may have the required magnitude. This eddy frictional dissipation is operating on the cloud scale. Vertical gradients of $\widetilde{v_r' w'}$ were determined with a two-layer model (i.e., estimates were made for the mid-tropospheric levels and zero values were assumed for the surface and the tropopause. This is a crude approximation, but it encourages one to seek further experimental data. With improved sampling and measuring techniques a reliable estimate of the importance of the $\partial/\partial z\,\widetilde{v_r' w'}$ term can be achieved. New instrumentation and special flight planning with National Hurricane Research Project aircraft is being contemplated for the 1961 and 1962 seasons with this purpose in mind.

* See Appendix for clarification of this point.

† Calculations performed in University of Chicago, meteorology laboratory class given by Prof. H. Riehl (1960).

## 4. Summary of principal results

The principal results from all of the levels within the four storms studies are :

(1). The gradient wind equation along the radial direction, as defined in this paper for hurricanes, does not express the radial balance of forces to a satisfactory degree of approximation in nearly all portions of the hurricane. The quantity $\dot{v}_r)_{gr}$ is nearly always a large fraction of the Coriolis and centrifugal acceleration. In some places $\dot{v}_r)_{gr}$ is even larger than these accelerations.

(2). Internal radial friction plays an important role in balancing the cyclindrical radial equation of motion. The frictional acceleration is directed towards the storm centre when $\dot{v}_r)_{gr}$ is positive and outward from the storm when $\dot{v}_r)_{gr}$ is negative. The average magnitude of the radial frictional acceleration for the 10 levels for which area integration could be performed is 25 to 30 per cent of the pressure gradient force and 35 to 40 per cent of the Coriolis and centrifugal acceleration. These internal radial frictional accelerations may possibly be accounted for by a vertical Reynolds stress term.

(3). All deepening or steady state hurricanes must have stronger pressure gradients than centrifugal and Coriolis accelerations in order to account for frictional dissipations.

(4). As a consequence of the large amounts of internal radial friction operating in the hurricane, the gradient wind equation in *natural* coordinates as well as the one in *cylindrical* coordinates can be in error by wide margins.

## 5. Conclusions

In this study the balance of forces in hurricanes has been examined along the radial direction in stationary and moving coordinates. The Coriolis acceleration proved negligible compared to the centrifugal acceleration as expected. But gradient or cyclostrophic balance, in general, is not achieved by a wide margin, both along the radial axis and in natural coordinates. The pressure gradient far exceeds that required to balance the centrifugal acceleration to the left, and falls somewhat short of the requirement to the right of the direction of motion. In moving coordinates this asymmetry is reduced but by no means eliminated. Hence the maximum wind may be interpreted as produced by ' overshooting ' toward low pressure far beyond the point of equilibrium. A similar situation appears to exist with respect to many extratropical wind maxima, especially high-speed centres along jet streams.

The field of radial motion shows general outflow ahead and inflow behind the hurricane. The zero line is to right and left of the direction of motion, approximately where the maximum difference between pressure-gradient force and centrifugal acceleration is found. This geometric relation is considered as more than coincidence and supports the preceeding deductions about the origin of the maximum wind.

The air is accelerated radially in the sense prescribed by the difference between pressure-gradient force and centrifugal acceleration. But the magnitude of the actual acceleration generally falls short of the computed acceleration by a wide margin. Hence it becomes necessary to postulate the existence of large lateral frictional forces which act opposite to the $\dot{v}_r)_{gr}$ accelerations. The magnitude is 0·1 to 1 dynes per unit mass which corresponds to a pressure gradient force of 1 mb/5 miles. Previously, such large frictional forces have not been suspected to exist. Nevertheless, there appears to be no valid reason *a priori* why the friction should not rise to become a substantially larger fraction of the pressure-gradient force in hurricane-type systems than under normal atmospheric circum-

stances. If so, an important limitation on hurricane development has been uncovered, and it remains for the future to give a quantitative expression to enter as a constraint in hurricane models.

## Acknowledgments

The author wishes to express his sincere gratitude to Professor H. Riehl under whose direction this paper was written. Professor Riehl proposed this topic, encouraged, and supervised all phases of its carrying out. The author also wishes to thank the National Hurricane Research Project and its past and present directors Messrs. R. Simpson, C. Gentry and H. Hawkins for generously furnishing the valuable data needed to make this study possible. The author expresses his appreciation to the U.S. Weather Bureau for providing financial assistance. Thanks are also due to Dr. T. N. Krishnamurti of the University of Chicago and the above mentioned Mr. R. Simpson for helpful discussions on this subject matter.

## References

Ausman, M. 1959 'Some computations of the inflow angle in hurricanes near the ocean surface,' Univ. of Chicago, Proj. Rep., (Unpublished manuscript).

Brunt, D. 1939 *Physical and dynamical meteorology*. Cambridge Univ. Press.

Haurwitz, B. 1941 *Dynamic meteorology*, McGraw-Hill, New York.

Hillary, D. T. and Christensen, F. E. 1957 'Instrumentation of Nat. Hur. Res. Proj. Aircraft.' *Nat. Hur. Res. Proj. Rep. No. 11*, U.S. Weather Bureau.

Hubert, L. F. 1959 'Distribution of surface friction in hurricanes,' *J. Met.*, **16**, p. 393.

Hughes, L. A. 1952 'On the low-level wind structure of tropical storms,' *Ibid.*, **9**, p. 422.

Jordan, C. L., Hurt, D. and Lowrey, C. 1960 'The structure of hurricane *Daisy* on 27 Aug. 1958,' *Ibid.*, **3**, p. 337.

La Seur, N. E. 1957 'An analysis of some detailed data obtained by aircraft reconnaissance of a hurricane,' *Contract Rep.*, Florida State Univ.

Malkus, J. S. 1958 'On the thermal structure of the hurricane core,' Proc. Tech. Conf. on Hurricanes, *Amer. Met. Soc.*

1959 'Recent developments in studies of penetrative convection and an application to hurricane cumulonimbus towers,' Tech. Rep. No. 6, Woods Hole Ocean. Instit., Unpublished manuscript.

1960 'Cloud patterns in hurricane *Daisy*, 1958,' Tech. Rep. No. 8, Woods Hole Ocean. Instit., Unpublished manuscript, p. 63.

Malkus, J. S. and Riehl, H. 1960 'On the dynamics and energy transformations in steady-state hurricanes,' *Tellus*, **12**, p. 1.

Miller, B. I. 1958 'Details of circulation in the high energy core of hurricane *Carrie*,' *Nat. Hur. Res. Proj. Rep. No. 24*.

Reynolds, O. 1895 'On the dynamical theory of incompressible viscous fluids and the determination of criterion,' *Phil. Trans. R. Soc., A*, **186**, p. 123.

Riehl, H. 1954 *Tropical meteorology*, McGraw-Hill, New York.

1959 'On production of kinetic energy from condensation heating,' *The Rossby-Memorial Volume*, and *Nat. Hur. Res. Proj. Rep. No. 22*.

Riehl, H. and Gentry, R. C. 1958 'Analysis of tropical storm *Frieda*,' *Nat. Hur. Res. Proj. Rep. No. 17*, p. 16.

Riehl, H. and Malkus, J. S. 1958 'On the heat balance in the equatorial trough zone,' Contribution to Palmen's 60th Birthday Volume, Geophsica, Helsinki.

Staff Members, Nat. Hur. Res. Proj. 1958 'Details of circulation in the high energy core of hurricane *Carrie*,' *Nat. Hur. Res. Proj. Rep. No. 24*.

Sherman, L. 1956 'On the wind asymmetry of hurricanes,' *J. Met.*, **13**, p. 500.

## Appendix

### (*1*). *Reliability of the computations*

The reader's first reaction to this study may be tinged with some scepticism as to the accuracy of the data and of the reliability of some of the computations made from the qualitative analysis. This may be particularly true of computations that made use of the radial wind component.

It must be emphasized that the Doppler navigation system, from which all the winds were obtained, is an extremely accurate navigation instrument. Winds above 10 to 15 kt are accurate to within two to three per cent in both direction and speed – except at isolated points in turn and in a few heavy rain areas. These areas were not used in the computations. The tangential wind components are just as accurate as the total wind.

All computations where $D$ values were used were dependent only on the gradient of the $D$ values and not on the absolute values themselves.

It should be remembered that the radial winds used in this study were those of the *actual radial wind* components and not the *relative radial wind* components. The magnitudes of the actual radial winds are much greater than the relative radial winds and lend themselves to far better evaluation.

Computations using the actual radial winds were made only from careful field analysis where isolated non-representative values could be disregarded and a relatively smooth well-defined pattern could be obtained. Evaluation of $\dot{v}_r)_{gr}$ and $\dot{v}_{rr})_{gr}$ were in no way dependent upon the radial wind.

That there may be a few inherent data and computational shortcomings in certain of the individual levels is not denied. The area integrations did require qualitative analysis. It is felt, however, that in the 10-level composites, these possible individual level shortcomings could not and did not disguise the broad-scale features displayed.

### (*2*). *Equality of frictional acceleration in fixed and moving storm centre* (*i.e.*, $F_{rr}$)

The substantial derivative relative to the moving storm centre – i.e., $\dot{v}_{rr}$ – is with the previous stated assumption of constant storm translation

$$v_{\theta r}\frac{\partial v_{rr}}{r\,\partial\theta} + v_{rr}\frac{\partial v_{rr}}{\partial r} + w\frac{\partial v_{rr}}{\partial z}$$

where $v_{\theta r}$ and $v_{rr}$ are the relative tangential and radial wind components. The local derivative $\partial v_{rr}/\partial t$ drops because of the steady state assumption. The relation between the substantial derivative with respect to the moving centre and that with respect to the *fixed centre* is then with the statement and footnote of the second paragraph of Section 3, (*1b*).

$$\dot{v}_{rr} - \left(-\frac{2v_\theta c_\theta}{r} + \frac{c_\theta^2}{r} - fc_\theta\right) = \dot{v}_r \quad . \quad . \quad . \quad (14)$$

Now

$$\dot{v}_r)_{gr} = \dot{v}_r - F_r, \text{ or } F_r = -[\dot{v}_r)_{gr} - \dot{v}_r] \quad . \quad . \quad . \quad (a)$$

$$\dot{v}_{rr})_{gr} = \dot{v}_{rr} - F_{rr}, \text{ or } F_{rr} = -[\dot{v}_{rr})_{gr} - \dot{v}] \quad . \quad . \quad . \quad (b)$$

and

$$\dot{v}_{rr})_{gr} = \dot{v}_r)_{gr} + \left(-\frac{2v_\theta c_\theta}{r} + \frac{c_\theta^2}{r} - fc_\theta\right) \quad . \quad . \quad . \quad (c)$$

$$\dot{v}_{rr} = \dot{v}_r + \left(-\frac{2v_\theta c_\theta}{r} + \frac{c_\theta^2}{r} - fc_\theta\right) \quad . \quad . \quad . \quad . \quad (d)$$

from previous stated principles and assumptions. Substituting (c) and (d) into Eq. (6)

$$F_{rr} = -(\dot{v}_r)_{gr} - \dot{v}_r) = F_r \quad . \quad . \quad . \quad . \quad (15)$$

The frictional acceleration with respect to the *moving* storm centre is thus shown to be identical with that with respect to the *fixed* instantaneous centre.